Supporting materials for—

Systematic investigation of the SERS efficiency and SERS hotspots in gas-phase deposited Ag nanoparticle assemblies

L. B. He,[a,b†] Y. L. Wang,[a] X. Xie,[a] M. Han,[b†] F. Q. Song, [b] B. J. Wang,[a] W. L. Chen,[c] H. X. Xu,[d] and L. T. Sun[a†]

a.   SEU-FEI Nano-Pico Centre, Key Lab of MEMS of Ministry of Education, Southeast University, Nanjing 210096, P. R. China

b.   National Laboratory of Solid State Microstructures, Nanjing University, Nanjing 210093, P. R. China.

c.   Department of Chemical Engineering, Monash University, Building 36, Clayton, Victoria 3800, Australia

d.   Centre for Nanoscience and Nanotechnology, School of Physics and Technology, and Institute for Advanced Studies, Wuhan University, Wuhan 430072, China

† Corresponding email for materials: L. B. He (helongbing@seu.edu.cn)

1. Number-density distribution of the Ag-RNBs fabricated on Formvar-filmed substrates

Taking into account all the nanoparticle bands, the mean diameter of the Ag nanoparticles deposited on Formvar-filmed substrates is around 10 nm. In the nanoparticle bands where particle number densities are quite high, the mean particle size slightly increases. **Figure S1** shows the band-dependent number density of the micro-Ag-RNBs fabricated on Formvar-filmed copper grids and silica slices. The number density initially increases rapidly and then turns to be slowly. It indicates that, when the Ag nanoparticle assemblies are nearly closely packed, further deposition will generate particle coalescence and growth rather than the increase of number density. Hence, on the bands with very dense Ag nanoparticles, the number density will even show a slight decrease. Thereby, the deposition mass is recorded and set as the threshold value to control the deposition process so as to avoid forming continuous films.
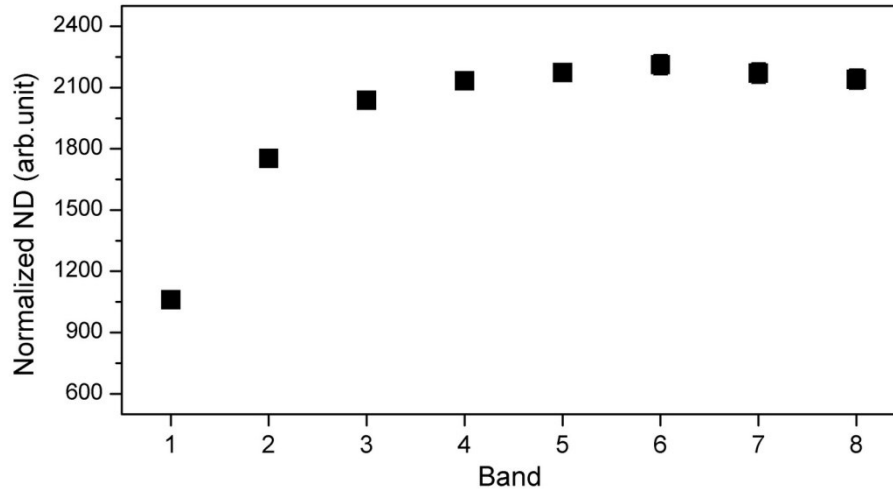
Figure S1. Band-dependent particle number density of the micro-Ag-RNBs presented in Figure 1.

2. Calculation of the inter-particle gaps

The inter-particle separations are calculated in a statistical way based on a large number of TEM images of each Ag nanoparticle band of the micro-Ag-RNBs. Typically, each of the Ag nanoparticles is firstly tracked pixel by pixel in the TEM images with the Digital Micrograph software, as shown in **Figures S2** (a)-(c). Then, all the Ag nanoparticles are numbered by the software. The mismarked nanoparticles are picked up manually, as shown in figures S2 (d)-(e). The edges of the Ag nanoparticles are tracked and put into a matrix and a script is programmed to calculate the nearest inter-particle spacing between each two neighboring Ag nanoparticles. A threshold value is set to only count the number of gaps with inter-particle separation less than it. **Figure S3** shows the illustration of inter-particle separations.
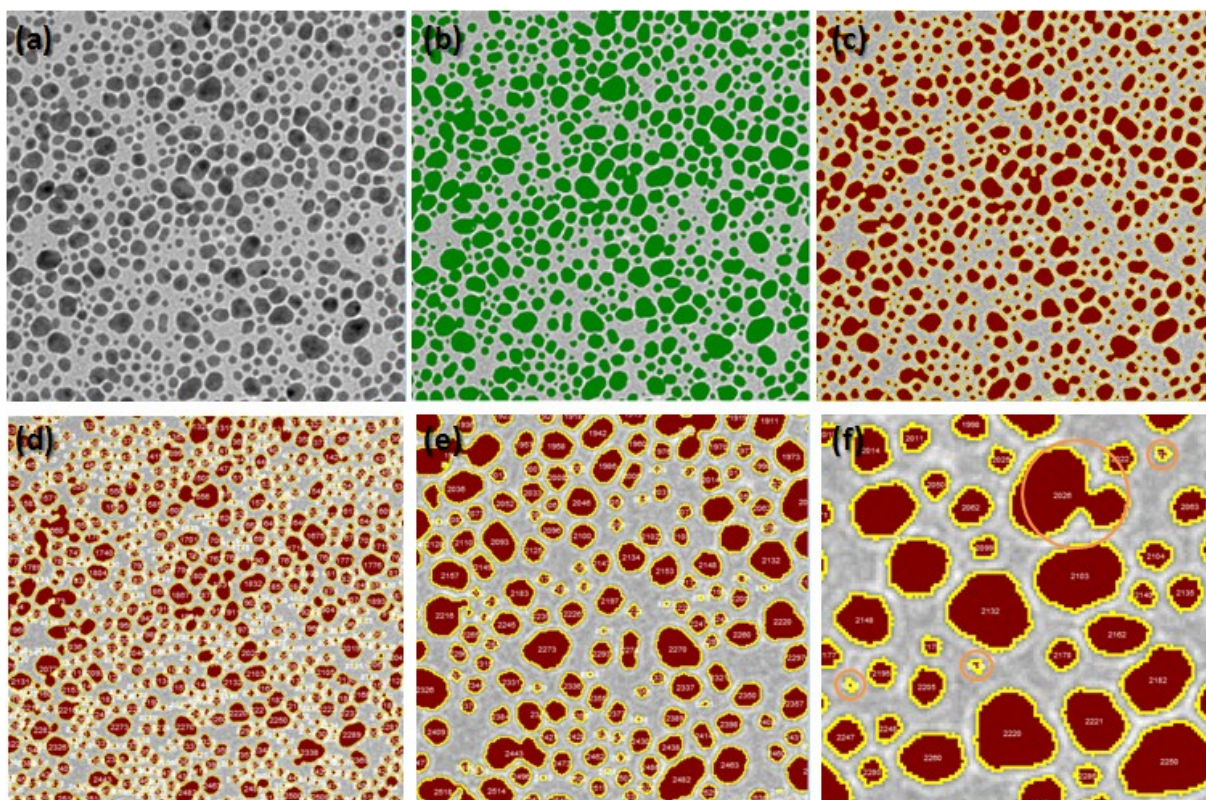
Figure S2. Illustration of the calculation of the inter-particle separations. **(a)** As-acquired TEM image of the Ag nanoparticle assembly. **(b)** Tracking of all the Ag nanoparticles by the Digital Micrograph software. **(c)** Identification of all the nanoparticles and their edges. **(d)-(e)** Marking all the Ag nanoparticles. **(f)** Marking the mismarked Ag nanoparticles for further calibration. The data of all the nanoparticle edges is collected and put into a data matrix for further analysis.
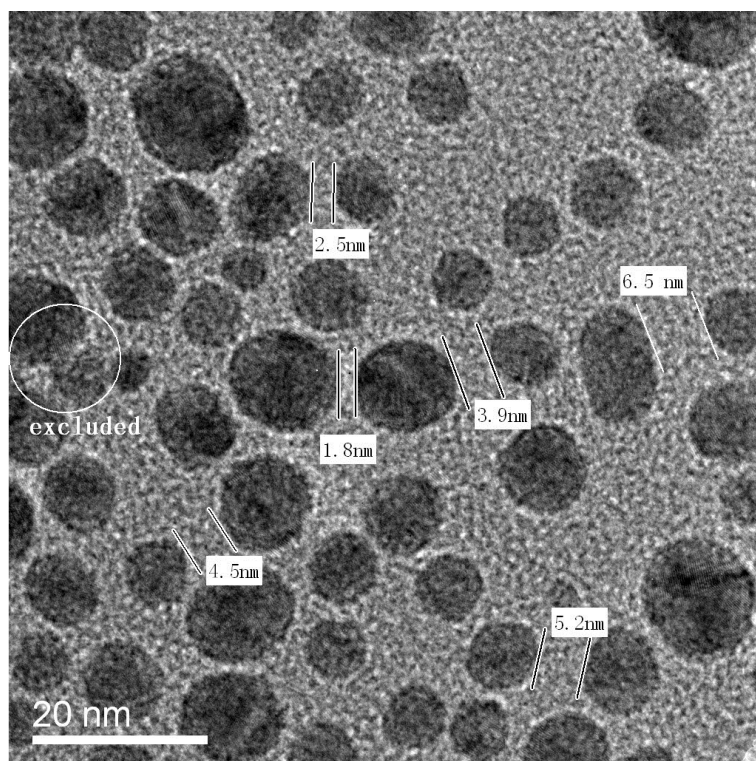
Figure S3. Illustration of the inter-particle separations between two neighbouring Ag nanoparticles. All the nanoparticle gaps are calculated from high-resolution TEM images by calculating the shortest spacing between each neighbouring nanoparticle pair.

3. SERS intensity distribution under a bi-laser excitation

Two lasers (i.e. 473 nm and 633 nm) are used to perform SERS intensity mappings on the same micro-Ag-RNBs. **Figure S4** shows the Raman intensity mapping monitored at 610 cm^{-1}. For the 473-nm excitation, the maximum intensity appears on band 5 counting from the lower side. For the 633-nm excitation, the maximum intensity shifts from the lower side to the upper side and appears on band 8.
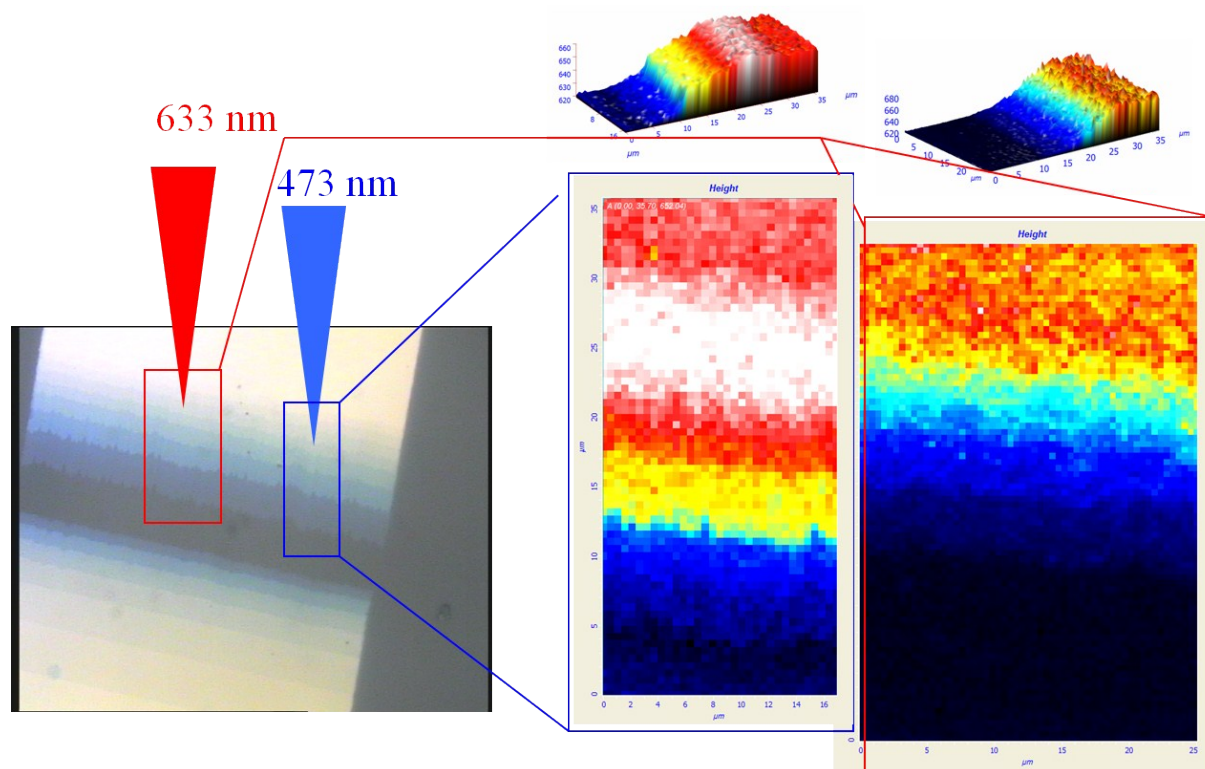
Figure S4. Intensity mappings of the Raman peak of R6G molecules at 610 cm^{-1} on the same micro-Ag-RNBs with excitation laser wavelengths of 473 nm and 633 nm, respectively.

4. Stepwise photo-bleaching of R6G molecules

As shown in **Figure S5**, the photo-bleaching is performed by stepwise scanning on the micro-Ag-RNBs with enlarging regions. A 473-nm laser is used and the laser powers used for photo-bleaching and SERS mapping are 1 mW and 100 μW, respectively.
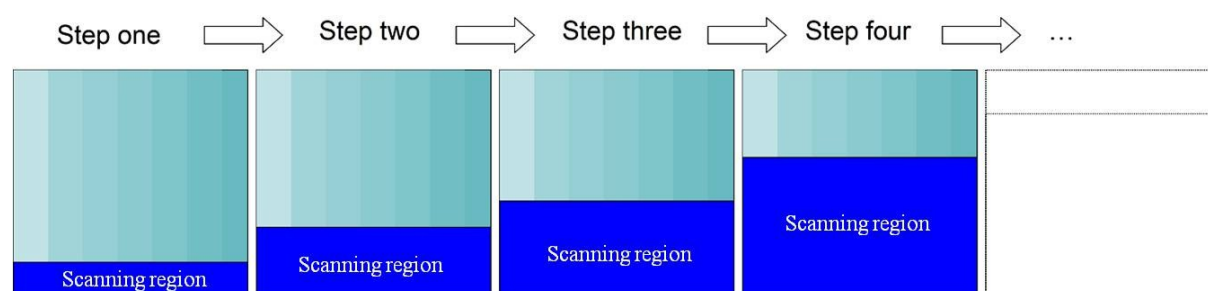

Figure S5. Schematic illustration of the stepwise photo-bleaching performed on the micro-Ag-RNBs. The turquoise bands represent the Ag nanoparticle bands while the blue regions indicate the scanning area for each photo-bleaching time.

5. Estimation of the molecule size effect

Two types of molecules, trans-1,2-di-(4-pyridyl) ethylene (BPE) and R6G, are selected to estimate the sensitivity of hotspots to molecule size. R6G and BPE solutions (both having a concentration of 5×10^{-6} M) are mixed and then dispersed on the micro-Ag-RNBs. SERS characterization is then performed and shown in **Figure S6**. In figure S6a, both the Raman fingerprints of BPE and R6G molecules are observed. By monitoring the characteristic Raman peaks (610 cm^{-1} for R6G and 1000 cm^{-1} for BPE), the intensity distributions of R6G and BPE molecules are acquired and shown in figure S6b. The maximum intensities of both these two types of molecules appear on band 5. It indicates that the molecule size effects can be neglected.
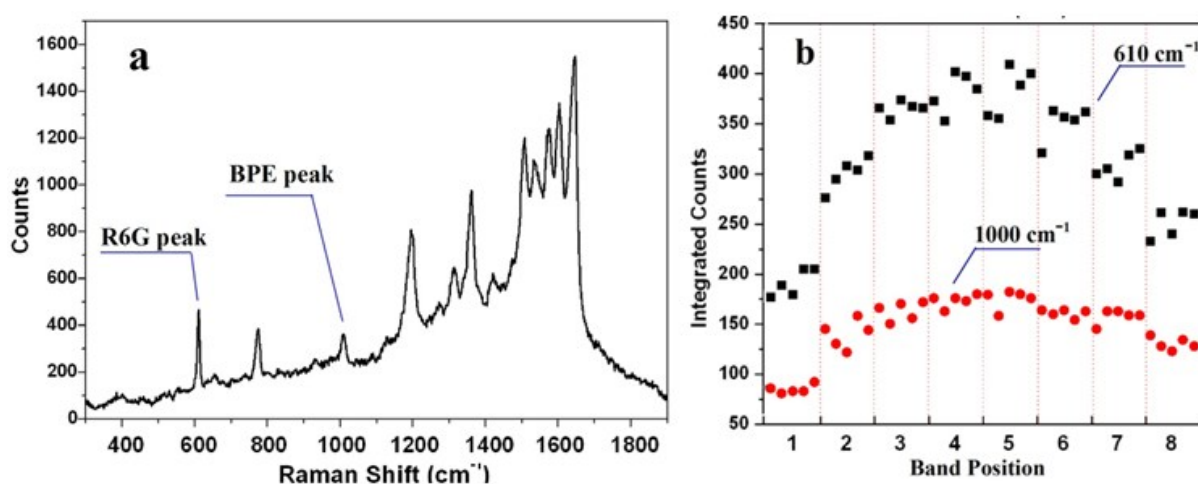

Figure S6. Sensitivity of hotspots to molecule sizes. **(a)** Raman spectrum of R6G and BPE molecules. **(b)** Band dependent Raman intensities of R6G and BPE molecules monitored at 610 cm^{-1} and 1000 cm^{-1}, respectively.

6. Illustration of the UHV-CBS for Ag nanoparticle deposition
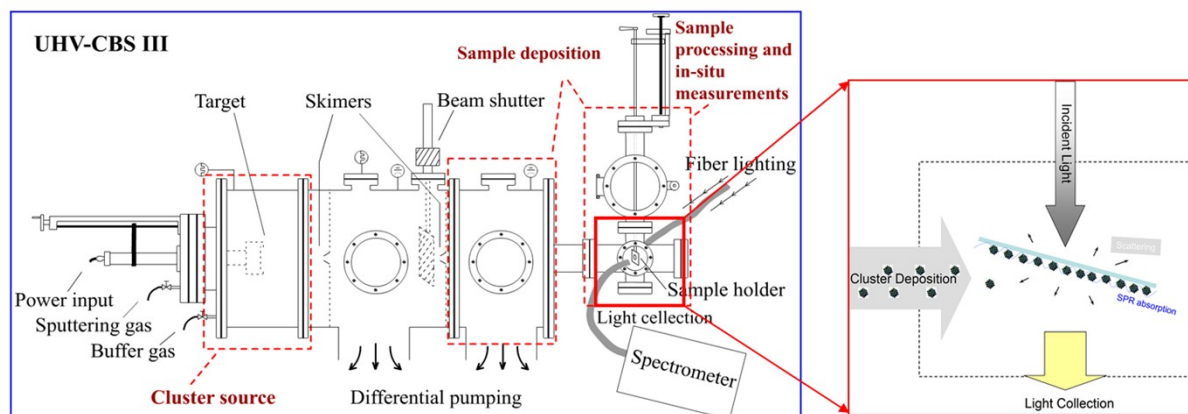

Figure S7. Illustration of the UHV-CBS configuration for deposition of Ag-RNBs.

7. Estimation of the SERS enhancement factor of Ag-RNBs

Figure S8 shows the mapping of a Ag-RNBs substrate by acquiring all the excited signals including Raman and photoluminescence (PL). In the Ag-RNBs, band 0 indicates a narrow band without any deposition of Ag nanoparticles. Bands 1-4 indicate regions with increasing deposition mass. The concentration of the R6G solution used is 10 μM and the experimental procedure is described in the experimental section of the manuscript. **Figure S9** shows the extracted spectra from the Ag-RNBs. As can be seen from both Fig. S8 and Fig. S9, the strong PL peaks make the contrast in Fig. S8 inverted in comparison to the Raman mapping in Fig. 2 in the manuscript. The broad PL peaks are retained as the reference for background subtraction. As can be identified in Fig. S9, Raman signal on band 0 (point 1) is rather undetectable. With the increase of deposition mass, the Raman signal increases remarkably (point 2 to point 5). Meanwhile, the PL continuously decreases possibly due to fluorescent quenching.
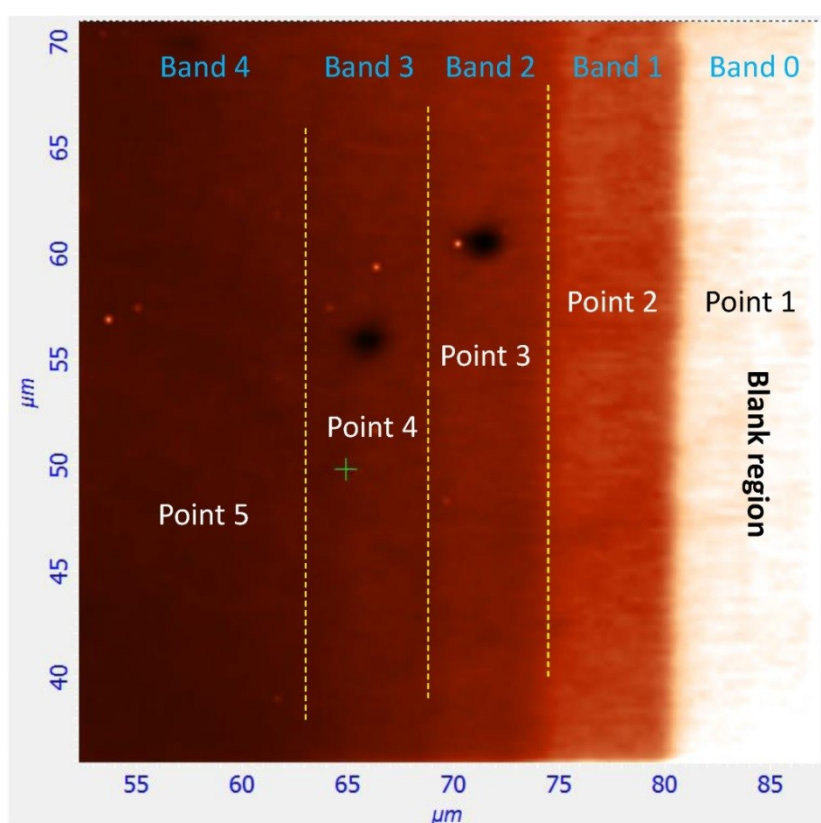

Figure S8. Mapping of the Ag-RNBs by acquiring the whole intensity from both Raman and PL.
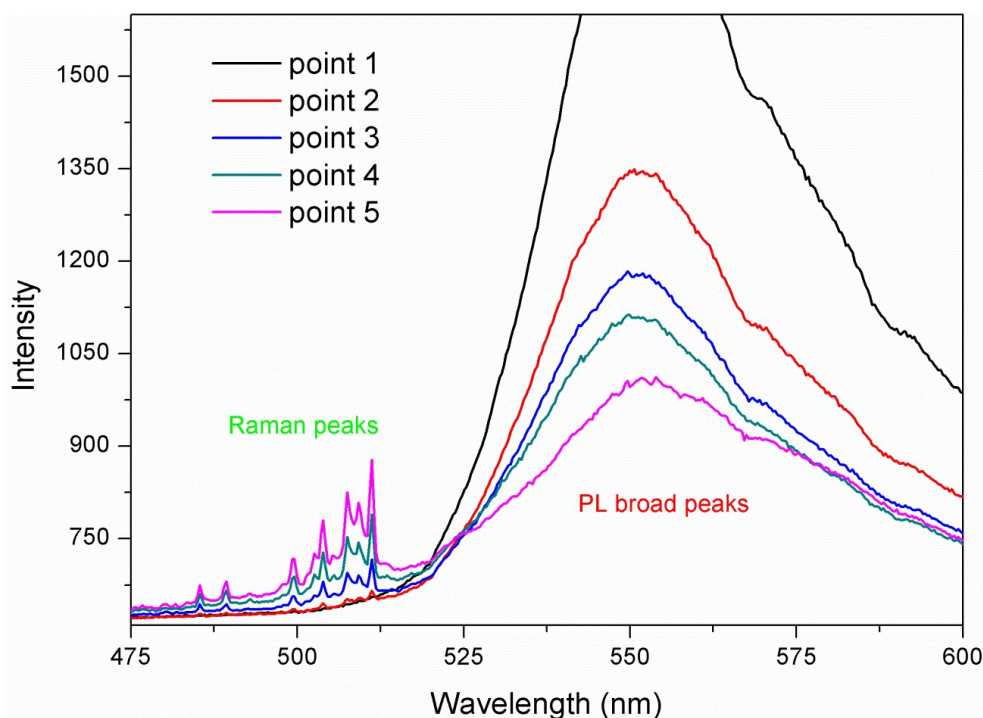
Figure S9. Extracted spectra from the points marked on the Ag-RNBs shown in Fig. S8.

For estimation of the SERS enhancement factor, a 100 mM R6G-in-methanol solution was used to prepare a reference sample. Typically, a drop (around 20 µL) of 100 mM R6G-in-methanol solution was dispersed onto a silica slice. For the Ag-RNBs substrates, each one was dispersed with a drop of 10 µM R6G-in-methanol solution. The samples were then dried under a nitrogen flow for Raman characterization. The laser power (473 nm) used on the Ag-RNBs substrates was 100 µW while the laser used on the silica slice substrate was 1 mW. With the same acquisition time, the maximum intensities of the Raman peaks were recorded. As typically shown in **Figure S10** for the comparison of the acquired Raman spectrum on a Ag nanoparticle band and the reference silica slice, the Raman signals were enormously enhanced. The enhancement factor was calculated roughly based on the intensities of the Raman fingerprints through the formula $\frac{I_{Ag-RNBs}}{I_{silica}} \times 10(laser-power) \times 10^4(concentration)$.

According to the measured maximum Raman intensties on different Ag-RNBs, the enhancement factors were estimated to be around 3.17×10^7 to 1.33×10^8.
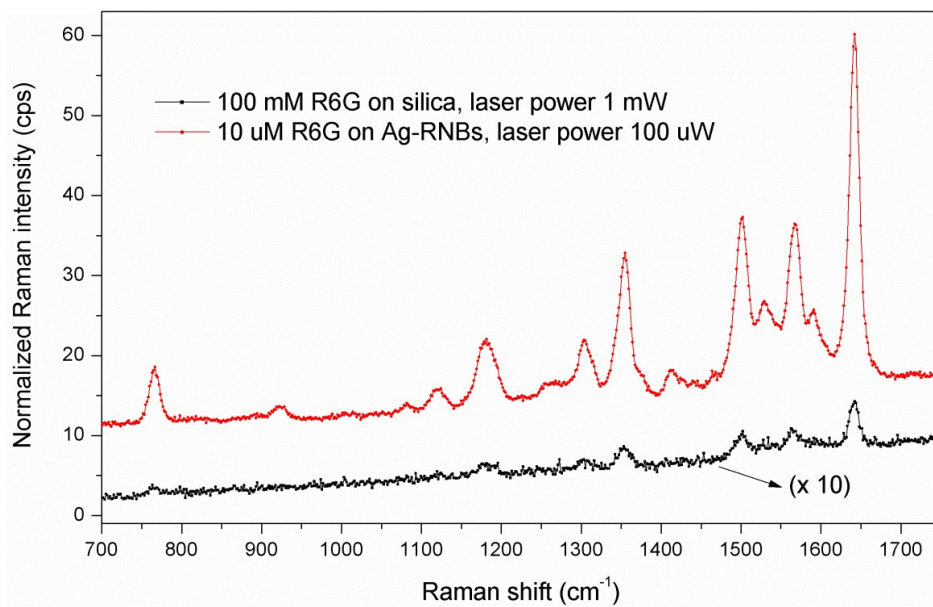
Figure S10. Raman spectra of R6G molecules dispersed on a Ag-RNBs substrate and a silica substrate respectively.